Journal of Biomedical Optics

SPIEDigitalLibrary.org/jbo

Localized cell stiffness measurement using axial movement of an optically trapped microparticle

Mary-Clare Dy
Shigehiko Kanaya
Tadao Sugiura

SPIE

Localized cell stiffness measurement using axial movement of an optically trapped microparticle

Mary-Clare Dy, Shigehiko Kanaya, and Tadao Sugiura
Nara Institute of Science and Technology, Graduate School of Information Science, Nara, Japan 630-0192

Abstract. A simple optical tweezers design is proposed to manipulate particles in the axial direction and estimate particle position with nanometer sensitivity. Balb3T3 cell is probed using two different-sized particles, and the localized cell stiffness is evaluated using Hertz model. A series of experiments are performed to obtain the necessary parameters for the cell stiffness computation: particle displacement, trapping stiffness, force exertion, and cell deformation. The computed cell stiffness measurements are 17 and 40 Pa using 4 μm- and 2 μm-sized particles, respectively. Results suggest that the proposed optical tweezers scheme can measure the stiffness of a particular cell locale using Hertz model, offering insights about how cells respond to outside mechanical stimulus. [DOI: 10.1117/1.JBO.18.11.111411]

Keywords: biomedical optics; biophotonics; microscopy; cells; image processing; optical tweezers; cell stiffness measurement.

Paper 130255SSPRR received Apr. 17, 2013; revised manuscript received Jul. 6, 2013; accepted for publication Jul. 11, 2013; published online Aug. 9, 2013.

1 Introduction

The mechanical studies on the cytoskeleton can provide important insights into the functions of biological molecules such as cell division, motility, mobility, growth of neuron cells and study of adaptive immune system[1,2] Specifically, mechanically stimulating the cytoskeletal components have been shown to play crucial roles in mediating and transferring subcellular local signals to the whole cell.[3] Optical tweezers are utilized to exert forces in the pN-order, which is suitable for studying the interacting forces between and within biomolecules,[4,5] the kinetics and properties of biological molecules,[6] and measurements of forces acting on particles in colloidal suspensions.[7,8]

Notable biological applications include stretching deoxyribonucleic acid (DNA), a red blood cell (RBC), and probing different types of cells; however, these optical traps are designed to move in the lateral direction.[9–11] Because cells move in three dimensions, examining the effects of exerted axial forces can elucidate more on the mechanical properties of cells. Studies that investigate axial forces utilize special devices such as acousto-optic modulators and spatial light modulators.[12,13] However, these works do not measure axial cell stiffness. Cell stiffness is primarily related to the cytoskeleton, which can reveal insights about cell structure and physiology. The proposed approach demonstrates an axial particle manipulation technique using 4 μm- and 2 μm-sized particles as probes to measure the stiffness of a Balb3T3 cell using Hertz model.

2 Experimental Setup and Methods

2.1 *Optical Tweezers Setup*

The optical tweezers setup in Fig. 1 is based on an inverted microscope (Eclipse T*i*-E, Perfect focus, Nikon Co., Japan). Using Nd:YAG laser ($\lambda = 1064$ nm, maximum output power = 4 W, Spectra Physics Lasers), a high numerical aperture 60× objective lens (NA = 1.2, Plan Apo WI, Nikon Co.) focuses the laser beam to create a single optical trap. A charged coupled device camera (WAT-902H, Watec Ltd., Japan) with shutter speed of 1 ms takes the images of the particles.[14] In dealing with cell samples, a wider field of view with reliable spatial homogeneity provided by image-based technique is necessary to obtain useful information.[15,16]

Axial particle manipulation in optical tweezers is performed by changing the laser spot position along the axial direction.[17] In the setup, the lens L1 is translated to vary the spot position. Figure 1(a) shows the axial particle displacement when lens L1, in Fig. 1(b), is translated. A LabVIEW program controls the stepping-motor translation of lens L1 and takes the particle images after each lens L1 step.

2.2 *Image Analysis and Position Estimation*

Particle position is based on the defocusing particle images as the particle is moved in the axial direction. To measure the apparent particle size, first, the particle is enclosed within the region of interest. Within this area, the threshold value is adjusted, and a local average filter further enhances the defocused particle image. Then, a circular edge detector searches through the image for sharp transitions in pixel intensities to obtain the best fit. A particle image taken at default lens L1 position is used as a basis for real-world units. Finally, the pixel coordinates of the particle images are transformed into the real-world coordinate through scaling in the x-(horizontal) and y-(vertical) directions.

A calibration graph is created to form a basis for axial particle position and z-focus position. The apparent size of a particle fixed on a glass slide is measured as a function of height of the objective lens, wherein the height is incremented using a piezoelectric stage (E-665.CR, PI GmbH and Co., Germany). The zero and maximum positions of the height of the objective lens encompass the subsequent change in apparent particle size when the lens L1 is translated for a given length. The linear equations of the corresponding calibration data are computed, and these equations relate the lens L1 translation with the

Address all correspondence to: Tadao Sugiura, Nara Institute of Science and Technology, Graduate School of Information Science, Nara, Japan 630-0192. Tel: 81-743-72-5321; Fax: 81-743-72-5329; E-mail: sugiura@is.naist.jp

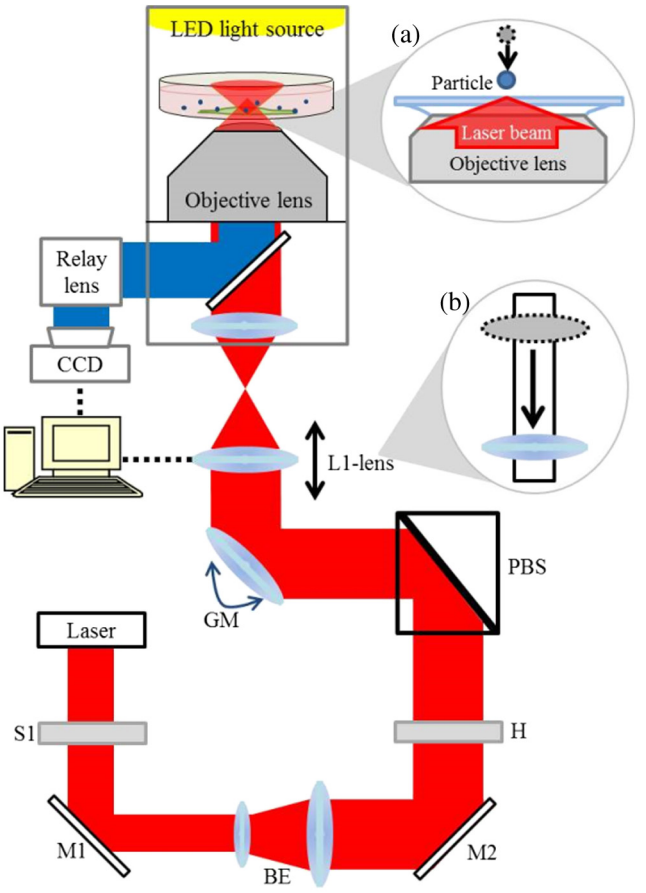

Fig. 1 Schematic diagram of the optical tweezers setup. Inverted microscope; S1: mechanical shutter; M1, M2: optical mirrors; BE: beam expander; GM: galvano mirrors; H: half wave plate, PBS: polarizing beam splitter. Inset: (a) Particle moves axially when (b) lens L1 is translated. Each lens L1 step corresponds to 100 μm.

axial particle position.[13] Finally, the z-focus position is computed by calculating the gradient of the axial position of an unattached particle as a function of lens L1. The system can detect 23 nm of change in axial particle position.

2.3 *Sample Preparation*

Each 4 μm- and 2 μm-sized polystyrene particles (Spherotech, Inc., USA) are diluted in distilled water and are placed on glass slides. Mouse fibroblast (Balb3T3) cells are cultured in Dulbecco's modified eagle medium supplemented with 10% fetal bovine serum, 1% penicillin, and streptomycin solution at 37°C and 5% CO_2. 80% confluent cells are treated with trypsin-ethylenediaminetetraacetic acid and are centrifuged at 1500 rpm for 5 min. The cells, after re-suspension in cultured medium, are placed in 35-mm glass bottom dishes treated with collagen. On the day of the experiment, the samples are washed with 2 mL buffer solution and fresh medium is added. 100 μL of diluted collagen coated particles (Micromod, GmBH, Germany) are added into the cultured samples.[14]

2.4 *Localized Cell Stiffness Computation*

In Hertz model, for a homogeneous, semi-infinite elastic solid, the force–displacement is determined by two material properties, the Young's modulus and Poisson's ratio. The force of the particle being exerted on a cell is related to the deformation depth δ by,

$$F_{\text{particle}} = \frac{4}{3}\frac{E}{(1-v^2)}R^{1/2}\delta^{3/2}, \tag{1}$$

where R is the radius of the probe, E is the Young's modulus and v is the Poisson ratio.[18]

Based on Eq. (1), $E/(1-v^2)$ describes the cell stiffness. The exerted force is computed using Hooke's law, $F = K\Delta z$, where K is the trapping stiffness and Δz is the shift of the particle from the laser focal position.[18]

The trapping stiffness is determined using Equipartition theorem,

$$K = \frac{k_B T}{\langle z^2 \rangle}, \tag{2}$$

where k_B is Boltzmann's constant, T is the absolute temperature, and z is the displacement of the particle from its equilibrium position. Based on Eq. (2), the trapping stiffness is inversely proportional to the positional variance of a trapped object.[16]

3 Results

To determine the axial trapping stiffness, the fluctuations or positional variance of a trapped particle as a function of laser power was measured. The laser power was measured at the exit of the objective lens to obtain a precise value of the laser power experienced by the particles. The trapped particle fluctuations became stable at different laser powers; for the 4 μm-sized particle at 37 mW laser power, the trapping stiffness was computed to be 4.5 μN/m. For the 2 μm-sized particle laser power at 24 mW resulted in trapping stiffness value of 11.4 μN/m. These laser power values were utilized for the axial displacements of unattached particles experiments and for the cell-attachment experiments.

For the unattached particle experiments, the position of the particle was set to 10 μm above the cover glass surface to be free from surface effect. Then the particles were moved upward and downward from a default lens L1 position. For the attached particle experiments, the trapped particle was positioned less than 4 μm away laterally from the boundary of the nucleus. The particle is placed near the nucleus to ascertain that the thickness of the cell sample will be much greater than the deformation to be created by the particle. The cell was then probed repeatedly to form an adhesion. Afterwards, the particle was moved upward, performing a "pull-up" motion. Sample images are shown in Fig. 2.

In Fig. 3, mechanical errors and Brownian motion experienced by the unattached particles provided discrepancy from a linear model. Also, as evident in Fig. 3(a), the axial position of the 4 μm-sized particle did not correspond to the z-focus position. Errors mainly caused by spherical aberration had possibly influenced the deviation of the particle position displacement from the z-focus position translation. In comparison, the inconsistency was not apparent in the smaller particle as seen in Fig. 3(b). The particles attached to the cell exhibited significantly fewer movements. The downward movement is analyzed further in the next paragraphs. On the other hand, the upward movement showed a gradual increase in particle displacement, suggesting that there was particle-to-cell adhesion. To verify the adhesion, after completing a set of upward motion,

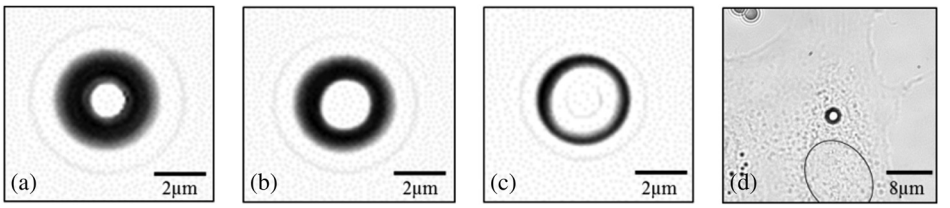

Fig. 2 Sample images of the 4 μm-sized particle moved in the axial direction. Unattached particle was moved downward with z-focus position at (a) default or 0 μm position, (b) 1.3 μm and (c) 2.5 μm. (d) An attached particle was placed on the cell surface near the nucleus (circled). The change in apparent size of the unattached particle is pronounced, as oppose to the attached particle that has barely perceptible change in apparent size.

the trapped particle was moved laterally using the stage. It was observed that at first, the trapped particle moved along with the stage, but afterwards, the particle sprung back towards the cell. It was also noted that tethers were formed between the particle and cell.

The Δz necessary to compute F_{particle} was computed from the shift of the particle from the laser spot position. When a particle is stably trapped and manipulated without obstructions, the laser focal position and the center of the particle are approximately in the same position. When the particle is attached to the cell, the particle is hindered by the cell to move further. This difference in the axial displacement of an unattached and attached particle was used to estimate Δz. Taking the trapping stiffness results mentioned earlier, a 4 μm-sized particle exerted a downward force of 9 pN and an upward force of 6 pN. A 2 μm-sized particle, on the other hand, exerted a downward force of 25 pN and an upward force of 14 pN.

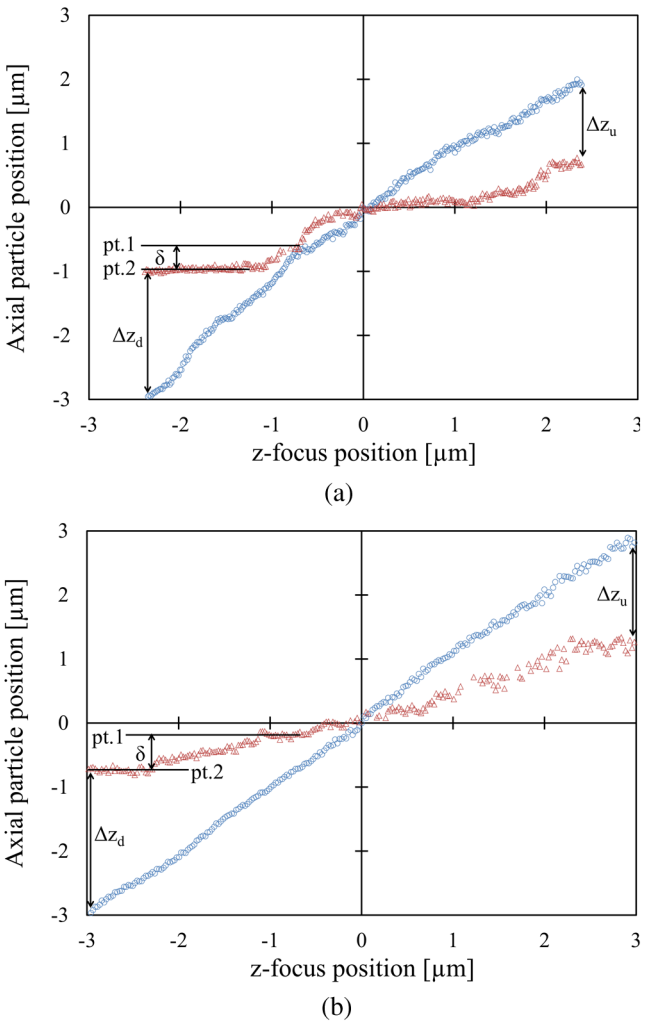

Fig. 3 Results from a single data set for axial displacement of (a) 4 μm-sized particle and (b) 2 μm-sized particle. The attached particle displacement (red triangles) had significantly less movement compared with the unattached particle displacement (blue circles). The Δz is measured as the difference in the unattached particle displacement and attached particle displacement. The cell deformation δ is estimated from point 1 to point 2 in the downward attached particle displacements.

For the cell stiffness computation, the cell deformation δ estimation is as follows: a particle is manually placed above the cell surface. From the default z-focus position, the particle is moved downward until it attaches to the cell surface at point 1, but no deformation is formed yet. From point 1, as the optical trap goes further down, force is applied on the cell thus creating the deformation. The graph is seen as having little change in the movement until point 2, at which the axial particle displacement becomes stable. The cell deformation was then estimated as the change in axial particle position from point 1 to point 2. The deformations were computed as 350 and 500 nm for the cell probed using 4 μm- and 2 μm-sized particles, respectively.

Now that the exerted forces, radii of particles, and deformations were taken into account, Balb3T3 cell stiffness was computed using Eq. (1), with Poisson ratio assumed to be 0.5 for soft biological materials.[19] The cell stiffness results were 17 and 40 Pa for the cell probed using 4 μm- and 2 μm-sized particles, respectively. The difference in the cell stiffness measurements was expected from the different probed cell locales and different cell samples. Because the cell structure is composed of different materials, it is expected that the mechanical behavior will also yield varying results. Given that the particles were situated within a range from the nucleus, the elastic modulus estimated over the region bounded by the smaller contact area resulted in greater value. The exerted force was also greater for the 2 μm-sized particle, and the deformation made was slightly larger than the deformation made using the 4 μm-sized particle. Further measurements of stiffness wherein the two different-sized particles are placed close to each other may offer more information regarding the effects of smaller probes in localized cell stiffness.

4 Discussion

Hertz model is used in atomic force microscopy (AFM) for the computation of the apparent stiffness of the cell.[18] Using AFM, the typical stiffness values of animal cells vary from 100 Pa to more than 10 kPa, with loading forces ranging from 100 pN to 1 nN.[20] The difference in the computed cell stiffness using optical tweezers and AFM is found in the measured force: one of the advantages of using optical tweezers is that it can measure forces in the lower range: 0.1 to 100 pN.[21] In this paper, the same motion as using an AFM and observing the Hertz model to

compute the cell stiffness was possible using optical tweezers. Traditionally, optical traps are used to attach particles on the cell and are moved laterally. The cell stiffness of RBCs was also computed using different models wherein the results vary from 2.5 to 200 μN/m.[4,22] There is yet no literature which suggests that the cell stiffness can be measured where the exerted force is performed axially using optical tweezers. Further work can be done to compute the pull-up cell stiffness, where the surface energy of both the attached particle and cell will be considered. Comparing the stiffness of healthy and unhealthy cells is also a possible application for the proposed system.

With the same length of z-focus translation, the linear regions in both the upward and downward displacements of trapped particles were determined. However, the difference in the upward and downward graphs of the unattached particle displacement may be due to spherical aberrations, viscous drag force, and mechanical errors. On the other hand, difficulty in the cell experiments is primarily caused by the distortion of particle movement due to repeated cell probing. Overall, when the axial movement of particles is being studied, the defocusing of the particles is observed. This means that the illumination of the particles, image analysis, and the stability of the system are important points to address. As a precaution, the experiments were carried out in series to decrease the probability of changing the illumination level. Then, for every new data set obtained, the image analysis program was recalibrated and rechecked with previous data sets. The ease of use of the system and minimum handling of the setup provided the opportunity to create a stable system, wherein the considerations lie in the mechanical drift of the objective lens and the stage, and the adjustment of laser power.

5 Conclusion

This paper proposed an axial manipulation system using optical tweezers. The system was used to measure localized cell stiffness of a Balb3T3 cell. 4 μm- and 2 μm-sized particles were trapped and manipulated in the axial direction. The unattached 4 μm-sized particle was translated for ≈ 5 μm, while the unattached 2 μm-sized particle was translated for ≈ 6 μm. The fluctuating movements of the trapped particle were also measured for the trapping stiffness using the proposed system, in which the trapping stiffness was greater for the 2 μm-sized particle. Experiments on cell attachments using pull-up and push-down motions were also performed. The reactive forces, which could provide insights on the cell stiffness, were computed. Finally, the cell stiffness was computed using the Hertz model, which had not been utilized before for the measurement of cell stiffness using optical tweezers. The push-down motion for the localized cell probing resulted in 17 and 40 Pa for the 4 μm- and 2 μm-sized particles, respectively.

Acknowledgments

We thank Dr. Kotaro Minato for valuable discussions and support of this work.

References

1. M. P. Sheetz, D. P. Felsenfeld, and C. G. Galbraith, "Cell migration: regulation of force on extracellular-matrix-integrin complexes," *Trends Cell Biol.* **8**(2), 51–54 (1998).
2. J. Dai and M. P. Sheetz, "Mechanical properties of neuronal growth cone membranes studied by tether formation with laser optical tweezers," *Biophys. J.* **68**(3), 988–996 (1995).
3. D. Ingber, "Tensegrity II. How structural networks influence cellular information processing networks," *J. Cell Sci.* **116(8)**, 1397–1408 (2003).
4. J. Sleep et al., "Elasticity of the red cell membrane and its relation to hemolytic disorders: an optical tweezers study," *Biophys. J.* **77**(6), 3085–3095 (1999).
5. F. M. Fazal and S. M. Block, "Optical tweezers study life under tension," *Nat. Photonics* **5**(6), 318–321 (2011).
6. M. Allioux-Guérin et al., "Spatiotemporal analysis of cell response to a rigidity gradient: a quantitative study using multiple optical tweezers," *Biophys. J.* **96**(1), 238–247 (2009).
7. C. O. Mejean et al., "Multiplexed force measurements on live cells with holographic optical tweezers," *Opt. Express* **17**(8), 6209–6217 (2009).
8. T. A. Nieminen et al., "Physics of optical tweezers," in *Methods in Cell Biology: Laser Manipulation of Cells and Tissues*, M. Berns and K. O. Greulich, Eds., pp. 207–236, Academic Press, San Diego, California (2007).
9. M. Dao, C. T. Lim, and S. Suresh, "Mechanics of the human red blood cell deformed by optical tweezers," *J. Mech. Phys. Solids.* **51**(11), 2259–2280 (2003).
10. A. Biebricher et al., "Tracking of single quantum dot labeled EcoRV sliding along DNA manipulated by double optical tweezers," *Biophys. J.* **96**(8), L50–L52 (2009).
11. L. Ikin et al., "Assembly and force measurement with SPM-like probes in holographic optical tweezers," *New J. Phys.* **11**(2), 023012 (2009).
12. T. Higuchi et al., "Three-dimensional positioning of optically trapped nanoparticles," *Appl. Opt.* **50**(34), H183–H188 (2011).
13. Y. F. Chen, G. A. Blab, and J. C. Meiners, "Stretching submicron biomolecules with constant-force axial optical tweezers," *Biophys. J.* **96**(11), 4701–4708 (2009).
14. H. Miyoshi, T. Sugiura, and K. Minato, "Cell palpation system based on a force measurement by optical tweezers for investigation of local mechanical properties of a cell membrane," *Jpn. J. Appl. Phys.* **48(12)** 120223 (2009).
15. S. Keen et al., "Comparison of a high-speed camera and a quadrant detector for measuring displacements in optical tweezers," *J. Opt. A—Pure Appl. Opt.* **9**(8), S264–S266 (2007).
16. M. Padgett, J. Molloy, and D. McGloin, *Optical Tweezers: Methods and Applications, Series in Optics and Optoelectronics*, Taylor and Francis Group, Boca Raton, FL (2010).
17. A. Ashkin et al., "Observation of a single-beam gradient force optical trap for dielectric particles," *Opt. Lett.* **11**(5), 288–290 (1986).
18. M. R. K. Mofrad and R. D. Kamm, *Cytoskeletal Mechanics: Models and Measurements in Cell Mechanics*, Cambridge University Press, New York (2006).
19. A. Touhami, B. Nysten, and Y. Dufrêne, "Nanoscale mapping of the elasticity of microbial cells by atomic force microscopy," *Langmuir*, **19**(11), 4539–4543 (2003).
20. M. Radmacher, "Measuring the elastic properties of living cells by the atomic force microscope," in *Methods in Cell Biology: Atomic Force Microscopy in Cell Biology*, B. P. Jena and J. K. Heinrich Hörber, Eds., pp. 67–90, Academic Press, San Diego, California (2002).
21. K. Neuman and A. Nagy, "Single-molecule force spectroscopy: optical tweezers, magnetic tweezers and atomic force microscopy," *Nat. Methods* **5**(6), 491–505 (2008).
22. G. Lenormand et al., "Direct measurement of the area expansion and shear moduli of the human red blood cell membrane skeleton," *Biophys. J.* **81**(1), 43–56 (2001).